A damping phenomenon in viscoelastic fluids

Xavier Frank, N. Dietrich, Huai-Zhi Li

A damping phenomenon in viscoelastic fluids

X. Frank, N.Dietrich and Huai Z. Li

Abstract– Flow fields behind a sphere settling in polymeric fluids are investigated using aParticle Image Velocimetry (PIV) technique. Complex features including both a negative wakeand a surrounding cone are quantified. In particular, an oscillation zone, which takes place behindthe negative wake, is identified for the first time. A physical understanding of various phenomenainvolved in the wake is gained. The damping phenomenon can be attributed to the viscoelasticproperties and the surrounding cone stems from a propagation frontof lateral viscoelastic waveemitted by the settling sphere. The oscillationfrequency and open angle of the surrounding coneare theoretically related to a viscoelastic Mach number. Satisfactory agreement with experimentsis observed.

Introduction. –The classical description of themechanical properties of fluids and materials at macro-scopic scale is usually based on two distinct behaviors:the viscous fluid [1] and the elastic solid [2]. However,most natural materials are viscoelastic and exhibit both.For example, Maxwell was among the pioneers to com-bine both basic concepts for the description of real ma-terials, such as the respective contribution of liquid andsolid according to applied stresses [3]. A central pa-rameter to be considered is then the relative time scalebetween deformation duration and materials' relaxationtime. When imposed deformations are long enough toallow stresses to relax, materials display simple viscousproperties. Otherwise, the application of deformationsis shorter than stresses' relaxation, materials behave asan elastic solid [4]. Since the early linear model ofMaxwell [3], viscoelastic fluids arose many intriguing ques-tions. Moreover, the viscoelastic character of fluids playsthe main role in such diverse fields as human tissues andpolymers [5], swimming microorganisms [6,7], volcaniceruption [8], decompression sickness [9], besides numerousindustrial applications [10].Among peculiar phenomena due to the viscoelastic-ity, the negative wake behind a settling sphere was ob-served for the first time by Hassager [11]. As the main flow pattern around a sphere settling in a purely viscousNewtonian fluid is downward in the neighborhood of thesettling axis, the flow behind a sphere settling in a vis-coelastic fluid can be surprisingly upward to form a so-called negative wake [12]. More recently, a global viewof such a wake was obtained by PIV measurements inthe case of polymer solutions [13], suspensions [14] andgels [15]. In all cases, the negative wake is largely ex-tended backward and is surrounded by a conical downwardflow zone. The question of the physical origin of the nega-tive wake gave rise to a controversial debate [12,16,17], themain role being successively attributed to various rheologi-cal features. Recently, a lattice Boltzmann model, coupledwith a simple linear rheological model, was able to repro-duce the main features of the flow [18], including the sur-rounding downward cone. This work clearly demonstratedthat the negative wake stems from the fluid's viscoelastic-ity, as it appears when the Deborah number, which is theratio between materials' relaxation time and deformationduration, reaches a threshold$De \geq 2$. When the nega-tive wake does exist, the opening angle of the surroundingdownward cone decreases with increasing sphere settlingvelocity, as observed in our previous experiments [13].However, the long-range behavior in the negativewake remains unexplored yet. Such a point is crucial inmany applications, as long-range interactions are respon-sible for bubble coalescences in chemical and biological reactors [19] and eruption violence in volcanoes [8], and lead to the structuration of particle suspensions in viscoelastic fluids [20]. The present work aims at capturing a better understanding of the flow pattern far away from the settling sphere.

Table 1: Parameters of rheological models in SI units.

Fluid	η_0	η_∞	λ	n	m'	n'
0.25%	10.80	0.041	26.4	0.268	28.12	0.538
0.50%	12.05	0.045	38.9	0.291	38.10	0.529
1.00%	33.31	0.070	65.1	0.303	67.83	0.558

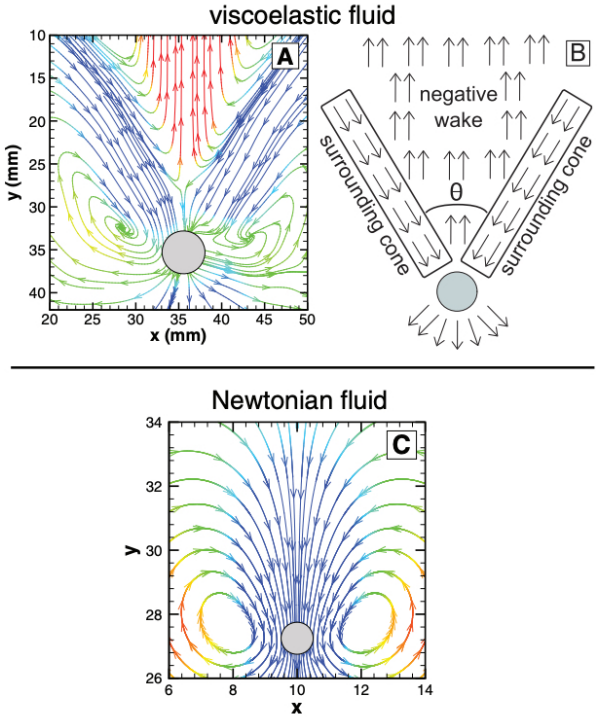

Fig. 1: (Color online) Streamlines of flow fields around a settling sphere. The sphere shape is added to guide the eye. Colors are related to the z component u_z of the fluid velocity $\vec{u}$: red for $u_z > 0$, blue for $u_z < 0$, green when u_z is close to 0. (A) Case of a viscoelastic fluid, from PIV measurement. The sphere diameter is $d_s = 5\,\mathrm{mm}$, the settling velocity is $v_s = 0.1\,\mathrm{m}\cdot\mathrm{s}^{-1}$, the sphere material is steel and the fluid is a 1% PAAm solution. (B) Schematic representation of the flow field around a sphere settling in a viscoelastic fluid. Negative wake, surrounding cone and cone's opening angle θ are drawn. (C) Case of a Newtonian fluid, from a lattice Boltzmann numerical simulation. The sphere diameter is $d_s = 1$, and the Reynolds number is set to $Re = 1$. Numerical results compare well with experimental data [14,23].

Experiments. – To investigate flow fields around a solid sphere settling in viscoelastic fluids, polyacrylamide (PAAm, AN 905 SH, SNF Floeger, France) solutions of three different concentrations, 0.25%, 0.5% and 1% (wt), were used. For a broad range of shear rates (˙γ = 0.01 to 500 s−1), the Carreau model η−η∞ η0−η∞ = [1 + (λγ˙)2] (n−1)/2 fits well the non-Newtonian viscosity η and a powerlaw model N1 = m [˙γ] n fits satisfactorily the first normal stress difference N1. Rheological parameters are summarized in table 1. Spheres of various diameters (5 to 20 mm) and materials (steel, glass and ceramic) were employed to reach a wide range of settling velocities in three square columns of various dimensions: 0.18 m large and 1 m high, 0.12 m large and 0.70 m high and 0.06 m large and 0.50 m high. Instantaneous velocity

fields around a settling sphere were measured using a PIV (Dantec Dynamics, Denmark) device with the help of fluorescent seeding particles with a mean diameter of 15 μm. Numerous experimental investigations through both the PIV and drag coefficient in this work demonstrate that a ratio superior to 10 between the column size and the diameter of settling spheres is required to ensure negligible effects of the column walls. This is relevant compared to the reported results in the literature such as [21]. The experiments presented in this work were then based on an optimal compromise between the following factors: the measurement accuracy and measuring windows of the PIV; fluid's nature; column size; spheres' diameter and related flow fields. This approach was also validated and tested with flow around a gas bubble of different shapes rising in viscous Newtonian fluids with a maximum error of 4.7% [22]. The PIV device allowed also the determination of the instantaneous velocity of a sphere at different positions in the column as well as its terminal settling velocity vs. Due to the relatively high value of the viscosity of fluids used, it was observed that the acceleration of a sphere was quickly absorbed by the fluids and the terminal settling regime was then reached after a travel of 0.1 m from the release point.

The flow fields around a sphere in the tested fluids have very peculiar features: the flow in the front of the sphere is very similar to that in the Newtonian case; in the central wake, the motion of the fluid is surprisingly upward in the opposite direction of the settling sphere; finally, a hollow cone of downward flow surrounds this negative wake. This conical downward flow zone begins on the sides of the sphere, and is largely extended backward (fig. 1(A), (B)). On the contrary, in the case of a Newtonian viscous fluid, the flow in the central wake is downward everywhere, as shown by a lattice Boltzmann simulation (fig. 1(C)) and experiments [14,23]. As the window size of the PIV is limited, we capture the long-range wake behind the settling sphere by continuously monitoring the flow fields after the leave of the sphere in an Eulerian framework. Besides the negative wake, another phenomenon not reported so far is observed: after the negative wake behind the sphere, a stagnant zone followed by another downward flow, and then again a stagnant zone followed by a new negative wake, and so on (fig. 2). This alternating pattern collapses progressively with increasing distance from the sphere.

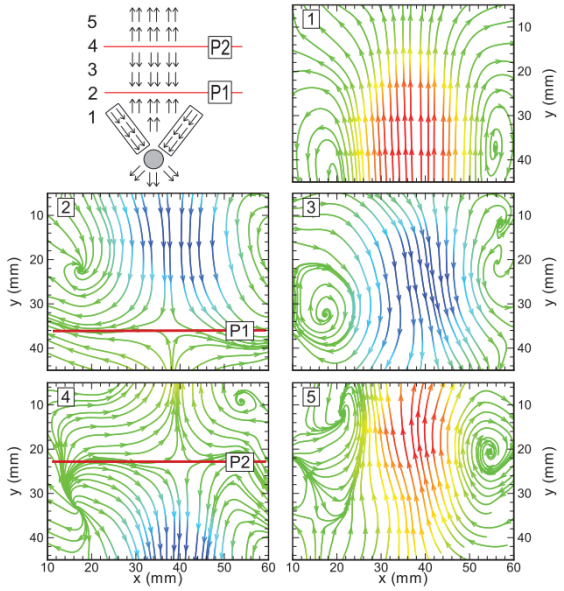

Fig. 2: (Color online) Successive captures of flow fields from PIV in a fixed window in the wake behind a 5 mm diameter steel sphere settling in a 1% PAAm solution. Colors are related to the z component of the fluid velocity $\vec{u}$: red for $u_z > 0\,\mathrm{m\cdot s^{-1}}$, blue for $u_z < 0\,\mathrm{m\cdot s^{-1}}$ and green when u_z is close to $0\,\mathrm{m\cdot s^{-1}}$. Top left: distribution of successive views in the wake. Planes $P1$ and $P2$, drawn as red lines, underline positions where $u_z = 0\,\mathrm{m\cdot s^{-1}}$.

The alternating pattern at the rear of the sphere can therefore be represented as a damped oscillation. To understand the physical origin of such an oscillator, a more quantitative approach is required. Clearly, only the axial component z of the velocity fields is relevant to characterize such an oscillator. According to an Eulerian description of the velocity fields, the temporary evolution of the z component is recorded in a fixed point behind the sphere's settling axis. The velocity variation exhibits a regular oscillation whose amplitude decreases with time and reaches zero as the settling sphere leaves away progressively from the measuring point (fig. 3). Obviously, observed damped oscillations are satisfactorily fitted by a linear Kelvin-Voigt model that is represented by a purely viscous damper and a purely elastic spring in parallel as shown (fig. 3). This implies that for the investigated range of viscoelastic fluids, a linear model can satisfactorily describe the damping phenomenon in the wake.

Discussion. – As shown in our earlier numerical experiments, the negative wake exists only in viscoelastic fluids [18]. An interpretation of such oscillations could be based on the consideration of fluid elasticity. Let us consider a local fluid strain as $\gamma \approx \delta$ rs , where rs is the sphere radius and δ a local fluid displacement. The resulting short-time viscoelastic stress can be deduced as $\approx G\gamma \approx G\,\delta$ rs , where G is the fluid's elastic modulus, and the volume force is $\approx G\,\delta$ rs2 . Assuming that ρ is the fluid density, the inertial force is $\approx \rho\, d2\delta\, dt2$ and the local force balance leads to the following simple harmonic equation: $d2\delta\, dt2 + G\,\rho$rs $2\,\delta = 0$. (1) A proper pulsation $\omega 0 = G\,\rho$rs2 can be deduced from eq. (1). Moreover, a shear wave propagation velocity $c = G\,\rho$ can easily be identified within this expression. The simplest dimensionless number that can be deduced from a wave propagation velocity is the well-known Mach number, which compares c and the translating source velocity vs, M = vs c = vs $\omega 0$rs . (2)

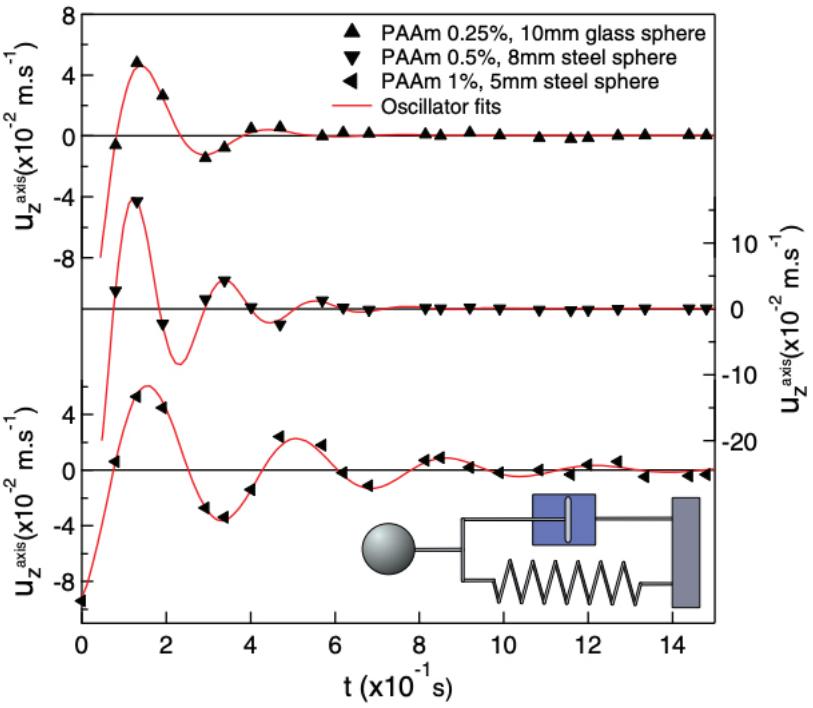

Fig. 3: (Color online) Examples of u_z oscillation at a fixed point on the settling axis after the sphere passage in a 0.25%, 0.5% and 1% PAAm solution, from top to bottom, respectively. The sphere diameter and the material vary with fluid and are included in each graph legend. Triangles are experimental data from PIV and curves are dissipative linear oscillator models $u_z\left(\vec{r}_0,t\right) = u_0 \sin\left(\sqrt{1-\sigma^2}\omega_0 t + \phi\right) e^{-\sigma\omega_0 t}$. The values of σ are 0.37, 0.21 and 0.16 for 0.25%, 0.5% and 1% PAAm, respectively.

Recently, shear waves were identified around a sphere settling in a viscoelastic fluid and sphere oscillations were attributed to reflection of such waves on column walls [24]. By means of both the PIV and the settling velocity to ensure a negligible effect of the column's wall, wave reflections on walls can be excluded as a major parameter in the presented damping results. Thus, oscillations in the wake can be identified as an intrinsic manifestation of fluid viscoelasticity. Shear waves are normally expected to propagate from the settling sphere towards column walls; however the fluid is viscous enough and the column width sufficiently large to dissipate a significant amount of mechanical energy in possible reflected waves. The downward hollow cone could find the physical origin in the propagation of such elastic shear waves. If such an assumption is justified, the opening angle θ should depend only upon M. To check this point, we perform Lattice Boltzmann (LB) numerical simulations [25–27]. In our previous work, a simple LB model, associated with a linear viscoelastic model for the fluid properties, is able to predict the apparition of a negative wake and a surrounding cone [18] as with a non-linear constitutive rheological model including shear-thinning behavior [13,28]. Along with the successful description of the damping velocity by the linear model (fig. 3), it is reasonable to argue that the main features of the fluid behaviour could be captured by a linear Maxwell equation. With a limited number of parameters, this approach aims at gaining the main contribution of elastic properties that seem to govern the damping phenomenon. This facilitates to some extent a straightforward comparison with experimental damping results that display

linear behavior, ∂τ ve i,j ∂t + 1 De τ ve i,j − 1 Reγ˙ i,j□ = 0. (3) The Deborah number is defined as De = trvs ds , where tr is the fluid relaxation time, which should be distinguished from the characteristic time λ used in the Carreau model, The Reynolds number is defined as Re = ρdsvs η , where η is the fluid viscosity, τ ve i,j , is the viscoelastic stress tensor, γ˙ i,j is the shear rate tensor and i, j are tensor indices. Our previous works reveal that both the Deborah number and the Reynolds number contribute to the negative wake in viscoelastic fluids. Instead of only the Deborah number, we make then use of a combination of both of them which is nothing but the Mach number easily deduced as M = √DeRe. As η = trG, this expression and the one from eq. (2) are clearly identical. Details of this model can be found in the original paper [18]. If the conical downward flow stems from the elastic wave propagation, its opening angle depends upon M and should not depend upon the Re-De couple when M is fixed. To adress such a point, two simulation sets with two fixed values of M2 = DeRe were carried out. Within each set, De is varied, the condition De > 2 being satisfied in order to give rise to a negative wake, and Re is easily deduced as Re = M2/De. Flow fields from the LB simulation (fig. 4(B)) exhibit both a negative wake and a surrounding cone, which compare favorably with PIV experiments (fig. 1(A)).

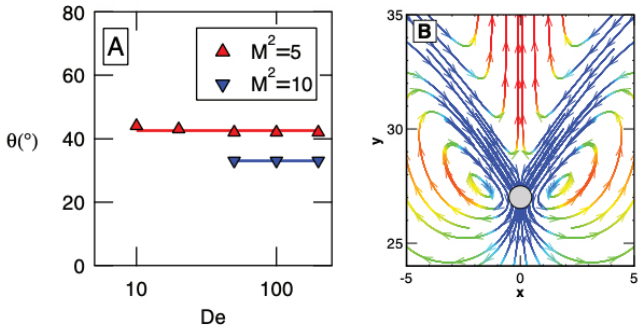

Fig. 4: (Color online) Results from LB simulations of a sphere settling in a viscoelastic fluid. (A) Opening angle of surrounding cone as a function of De for two values of $M^2 = DeRe$, horizontal lines are added to guide the eye. (B) Example of streamlines of the flow field from the LB simulation ($M = 2$), colors are related to the z component u_z of the fluid velocity $\vec{u}$: red for $u_z > 0$, blue for $u_z < 0$, green when u_z is close to 0. The flow pattern is presented by streamlines in satisfactory agreement with experimental results (fig. 1(A)).

Numerical simulations reveal that θ depends only upon M (fig. 4(A)) and corroborate the hypothesis that the surrounding cone is a viscoelastic wave front emitted by the settling sphere. Experimental values of M range from ≈ 0.3 to ≈ 3, and conical shockwaves are expected in flow fields only for M > 1. A conical shockwave opening angle can then be deduced from a Mach number, using the relationship sin (θ/2) = 1/M when M > 1. However, no qualitative difference appears in experimental results when the threshold occurs from M < 1 to M > 1. This confirms that a shockwave origin can be excluded. The hollow cone emerges from the propagation of elastic shear waves towards column walls, but cannot be identified as a shockwave. Shear rate at the surface of a sphere slowly translating in a fluid is not homogeneous. In the purely viscous fluid case, the maximum value of shear rate is mainly located at equatorial zones, according to the wellknown potential flow theory. According to our experimental PIV measurements and the LB simulation, this flow pattern around the sphere's equatorial zone is quite similar between viscoelastic and Newtonian fluids. We can argue then that shear waves are essentially emitted from the sphere's equatorial zone. The fluid is sheared

in vertical direction, and, consequently, transversal shear waves propagate in horizontal direction, orthogonally to its vertical translating axis. As the source is translating during wave emission, the wave front forms a conical shape, whose opening angle depends upon wave propagation velocity c and sphere settling velocity vs through the viscoelastic Mach number M. If we consider a Δt time interval, the settling distance during such an interval is $vs\Delta t$ and the wave propagation distance is $c\Delta t$. We can identify $vs\Delta t$ as the cone height and $c\Delta t$ as the cone radius. The angle θ can be easily computed as $\tan \theta 2 = 1 M$. (4) According to our earlier experimental investigations, the opening angle of the cone θ depends upon the sphere's settling velocity, the cone is widely opened ($\theta \approx 180^\circ$) for a slow settling sphere, and θ decreases as the sphere velocity increases [13]. Such results could be easily explained following eq. (4) as the viscoelastic Mach number M increases with the sphere's velocity vs. Using eq. (2), a value of M can be deduced from experiments. Then, experimental results can be satisfactorily described by this theory (fig. 5). As illustrated in fig. 5, experimental data and LB simulations are in good agreement with the prediction of eq. (4). The opening angle value is close to $\theta \approx 180^\circ$ for low values of M, and decreases with increasing M. It is worth distinguishing the lateral wave propagation from elastic shock transverse waves [29] or sonic boom [30]. In spite of an agreement when $M > 2$, the surrounding cone simply does not exist for $M < 1$ according to the shockwave theory. On the contrary, the lateral wave propagation theory describes satisfactorily the whole investigated range of M, in particular for $M < 1$. As a consequence, a better understanding is gained for the complex wake behind a sphere settling in viscoelastic fluids. Spheres translating in these fluids induce a shear, whose propagation towards column walls provokes a hollow cone. As viscoelastic stresses created by the shear relax progressively in fluids, a damping phenomenon takes place in the wake through a slowly dissipated viscoelastic oscillation. There is no direct causal relationship between damped oscillations in the wake and the hollow cone.

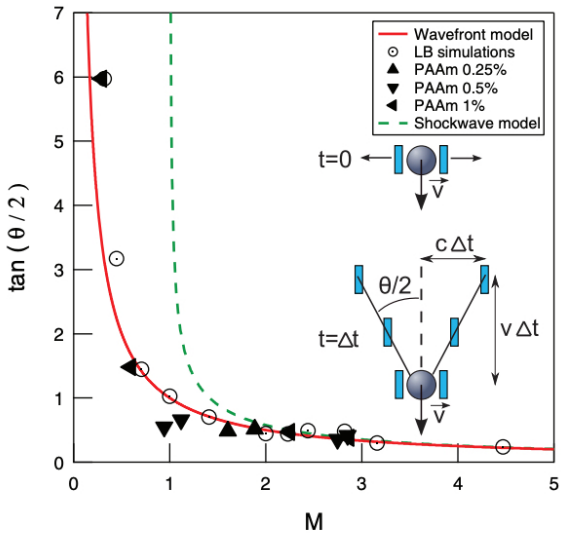

Fig. 5: (Color online) Downward flow cone opening angle θ as a function of Mach number M. Full symbols: data from experiments with 0.25%, 0.5% and 1% PAAm solutions and various sphere diameters and materials. Empty symbols: data from LB simulations. The determination of an angle for opening cones is not easy when the angle value is small. This is true for both the experimental flow fields measured by the PIV and the LB simulation. Small fluctuations observed can be attributed to this difficulty. The solid curve is the prediction from the lateral wave propagation theory (eq. (4)) and the dashed line is the prediction from shockwave theory: $\sin(\theta/2) = 1/M$ for $M > 1$. Inset: schematic representation of the lateral wave propagation theory. Two fictitious steps are drawn, at $t = 0$ and $t = \Delta t$ dates. Shear waves, schematically drawn as rectangles, are emitted from the sphere and propagate towards column walls while the sphere settles down. The half-angle $\frac{\theta}{2}$, shown in the inset, is the angle between the wave front and the settling axis.

While both the damped oscillations in the wake and hollow cone emerge from the fluids' elasticity, a reliable correlation can be drawn between these phenomena. Concretely, the damped oscillations and the hollow cone are both related to the elastic shear wave velocity c = G ρ , through the proper pulsation ω0 on the one hand, and the viscoelastic Mach number M on the other hand. We have tried to assess quantitatively a possible analytical relationship between the damping frequency and experimental rheological data such as the relaxation modulus issued from a rheometer. The main difficulty arises from the length-scale–dependent rheology of polymer solutions that has yet to be fully described [31]. In a recent work reporting micro-macro-discrepancies in nonlinear rheology [32], it is recognised that the Lagrangian unsteady forcing experienced by material elements in response to the moving colloidal probe for active microrheology induces spatial inhomogeneity of the strain rate. The resulting microrheology reflecting the bulk microstructure differs qualitatively and quantitatively from the macroscopic rheology. The damping frequency is determined by local solicitations at microscale exerted by a solid sphere, similar to a colloidal probe employed in characterizing microrheology. However, our experimental data concerning the relaxation modulus is a macroscopic parameter, measured by means of a standard geometry like Couette's on the rheometer in an integral manner for the whole measuring sample. A modulus G at microscale would be required to allow a possible scaling as the rheological properties are sensitive to the length scales that determine both network structure and filament orientation of polymers in solution. Conclusion. – In summary,

we throw new insight into the long-range wake behind a sphere settling in viscoelastic fluids. Both negative wake, in which the fluid flows upward contrary to the settling sphere, and its surrounding cone taking place around the negative wake, were amply demonstrated. In particular, we identify for the first time a zone just behind the negative wake in which oscillations appear. A linear dissipative oscillator model fits well the vertical component of fluid velocity in this new zone. Clearly, we show that oscillations in the wake can be attributed to the viscoelasticity of the fluid, and deduce then a viscoelastic Mach number. Furthermore, we demonstrate that the surrounding cone arises from the lateral propagation of a shear wave with respect to the settling axis, the sphere being the translating source. The experiments validate this proposal. These results could provide a benchmark solution for both academic and industrial studies where viscoelastic fluids are involved.

REFERENCES

[1] Newton I. S., in Philosophiae Naturalis Principia Mathematica, edited by Pepys S. (Royal Society, London) 1686.
[2] Hooke R., De Potentia Restitutiva, edited by Martyn J. (Royal Society, London) 1678. [3] Maxwell J. C., Philos. Trans. R. Soc. Lond., 156 (1866) 249. [4] Nosenko V., Goree J. and Piel A., Phys. Rev. Lett., 97 (2006) 115001. [5] Lakes R., Viscoelastic Materials (Cambridge University Press, Cambridge) 2009. [6] Teran J., Fauci L. and Shelley M., Phys. Rev. Lett., 104 (2010) 038101. [7] Gagnon D. A., Shen N. and Arratia P. E., EPL, 104 (2013) 14004. [8] Manga M. and Loewenberg M., J. Volcanol. Geotherm. Res., 105 (2001) 19. [9] Gault K. A., Tikuisis P. and Nishi R. Y., Undersea Hyperbaric Med., 23 (1995) 249. [10] Chhabra R. P., Bubbles, Drops, and Particles in Non-Newtonian Fluids (CRC Press, Boca Raton) 2006. [11] Hassager O., Nature, 279 (1979) 402. [12] Arigo M. T. and McKinley G. H., Rheol. Acta, 37 (1998) 4. [13] Kemiha M., Frank X., Poncin S. and Li H. Z., Chem. Eng. Sci., 61 (2006) 4041. [14] Gueslin B., Talini L., Herzhaft B., Peysson Y. and Allain C., Phys. Fluids, 18 (2006) 103101. [15] Mougin N., Magnin A. and Piau J. M., J. Non-Newtonian Fluid Mech., 171-172 (2012) 42. [16] Harlen O. G., J. Non-Newtonian Fluid Mech., 108 (2002) 411. [17] Dou H.-S. and Phan-Thien N., Rheol. Acta, 43 (2004) 203.
[18] Frank X. and Li H. Z., Phys. Rev. E, 74 (2006) 056307.
[19] Li H. Z., Frank X., Funfschilling D. and Mouline Y., Chem. Eng. Sci., 56 (2001) 6419.
[20] Michele J., Patzold R. ¨ and Donis R., Rheol. Acta, 16 (1977) 317.
[21] Chhabra R. P. and Uhlherr P. H. T., Can. J. Chem. Eng., 66 (1988) 154.
[22] Frank X., Funfschilling D., Midoux N. and Li H. Z., J. Fluid Mech., 546 (2006) 113.
[23] Tatum J. A., Finnis M. V., Lawson N. J. and Harrison G. M., J. Non-Newtonian Fluid Mech., 127 (2005) 95.
[24] Tabuteau H., Sikorski D. and De Bruyn J. R., Phys. Rev. E, 75 (2007) 012201.
[25] Succi S., The Lattice Boltzmann Equation for Fluid Dynamics and Beyond (Clarendon Press, Oxford) 2001.
[26] Qian Y. H., d'Humieres D. and Lallemand P., Europhys. Lett., 17 (1992) 479.
[27] Giraud L., d'Humieres D. and Lallemand P., Europhys. Lett., 42 (1998) 625.
[28] Frank X. and Li H. Z., Phys. Rev. E, 71 (2005) 036309.
[29] Catheline S., Gennisson J.-L., Tanter M. and Fink M., Phys. Rev. Lett., 91 (2003) 164301.
[30] Bercoff J. B., Tanter M. and Fink M., Appl. Phys. Lett., 84 (2003) 2202.
[31] Liu J., Gardel M. L., Kroy K., Frey E., Hoffman B. D., Crocker J. C., Bausch A. R. and Weitz D. A., Phys. Rev. Lett., 96 (2006) 118104.
[32] De Puit R. J. and Squires T. M., J. Phys.: Condens. Matter, 24 (2012) 464106.